Fiber sensing tuned by shape deformation and surface plasmon polariton

LI JIANGYAN[a,*], XIA CHUNMEI[a], WANG YUFEN[a], GAO LIHUA[b]
[a]*Departerment Of Information engineering, Binzhou University, Binzhou, Shandong Province, China*
[b]*Bincheng District No. 5Middle School, Binzhou, Shandong Province, China*

We have simulated the transmission spectra for the tapered fibers with no, one and two deformations in the visible wavelength range by Finite-Difference-Time-Domain method. The transmission peak positions shift to the shorter wavelength and the intensity changed to be larger, when the taper is added to the fiber or the taper deformation changed to be larger. The deform sensitivity for the tapered structures with different taper diameter is about 1.59e-3 nm·μm-1. The interference structure is apparent in the electric field distributions and there is apparent interference stripes in the interference structure. The transmission spectra for the tapered fiber immersed in different refractive media are present. The refractive sensitivity for the fiber with two deformation is about 50 nm/RIU and for the one tapered fiber is about 12.3 nm/RIU. The visible tapered fiber can be extensively applied to the bio-chemical sensor and physical test and so on.

(Received October 10, 2020; accepted October 7, 2021)

Keywords: Tapered fiber, sensor, transmission spectra

1. Introduction

Fiber sensor has been widely studied for applications in bio-chemical detection [1-5], environment monitoring [6-8] and physical test [9-11]. Tapered fiber is one kind of the fiber which form the deformation by the special processing technology [12-15]. With the special processing technology, the fiber is firstly heated and then carefully trenched. The fabricated tapered fiber has a small diameter down to nanometer scale at the heated region which support strong evanescent field at the fiber surface [16-18]. Micro-meter fiber is sensitive to the environment disturbance based on the interaction between propagating light and surrounding medium. The optical loss is about 0.01 dB/mm for the micro-fiber with the diameter 50 nm. The sensitivity for 400 nm diameter micro fiber Mach-Zehender sensor is about one order higher than that of the micrometer fiber sensor [19-20]. These fiber sensors and micro-fiber can be extensively applied to the light integration circuit, bio-chemical sensor and physical test. Due to the smaller width of the tapered fiber, the tapered structure is more sensitive to detect the surrounding environment media and physical deformation. The sensitivity is changeable relying on the deformation number, deformation parameter and the deformation structure shell diameter [21-27].

In this paper, the simulated transmission spectra of the tapered fiber in the visible wavelength range are presented based FDTD method. The transmission peak positions are sensitive to the taper number and the taper parameter and the sensitivity is about 1.59e-3 nm·μm-1 for the tapered fiber. Interference structure exist in the electric field distribution and interference stripes are also apparent. The interference structures are more apparent for the tapered fiber than that of the common fiber. The sensitivity of the one tapered fiber and the two tapered fiber to the surrounding environment refractive is different. The two tapered fiber is more sensitive than that of the one tapered fiber and is about 50 nm/RIU in the visible wavelength range. The sensitivity of the one tapered fiber is about 12.3 nm RIU-1 in the visible wavelength range. There is light self-focus at the outlet of the fiber in the electric field distributions images for the tapered fiber. The electric field

at the focus is about 30 times larger than the incident electric field and the focus diameter is about 200 nm. There is also interference structures in the electric field images of the no tapered fiber due to the smaller the fiber length and the interference is more apparent in the electric field distribution images for the two tapered fiber.

2. Results and discussion

We employ FDTD method to calculate the optical transmission spectra and near-field distribution at the surface of the fiber outlet under the normal incidence of infrared plane-wave light from the bottom side of the fiber. In the simulation we have noticed the two-fold mirror reflection symmetry involved in the structure and taken into full account such geometric features to significantly save memory space and computational time. In addition, the dispersion data (including the real and imaginary parts of permittivity) of gold have been used in the simulation. As such, the absorption effect of metal materials has been automatically taken into account. In the simulation, we have used 5 nm as the mesh grid.

The considered tapered fiber structure and the fiber sensor principle are shown in Fig. 1. The diameter of the fiber core is 3 μm and the diameter of the fiber shell is about 6 μm. The refractive of the fiber core is 1.465 and it is 1.46 for the fiber shell. The length of the fiber is finite, which introduces the electric field interference reflected by the entrance and outlet. We have fabricated the taper on the fiber by the special process technology and the taper structure is similar to the common fiber. The core diameter of the taper is about 1.5 μm and the shell diameter is about 3 μm and the deformation length is about 0.4 μm. The taper structure for the two tapered fiber is also same with that of the one tapered fiber. The light emerged from the laser propagates along the incident fiber and detected by the detector after going through the sensor. The light propagates along the Z-axis and polarized along x-axis shown in Fig. 1.

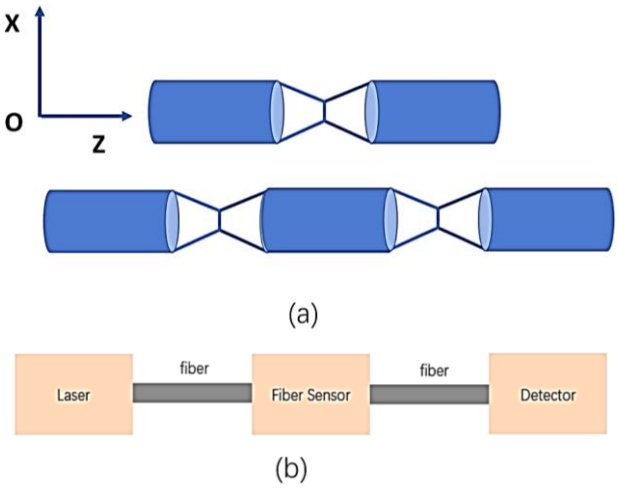

Fig. 1. (a) The considered taper fiber structure with deformation. (b) The light path image for the taper fiber sensor. The light emerged from the laser propagates along the incident fiber and detected by the detector after going through the sensor (color online)

The simulated transmission spectra for the tapered fiber by use of Finite-Difference-Time-Domain methods in the visible wavelength range are shown in Fig. 2. The light is incident along the fiber-axis direction and polarized in the radiant direction. Transmission peak and transmission dip exist in the transmission spectra in the visible wavelength range. The transmission amplitude for the transmission peak is about 0.17 for the tapered fiber with the taper deformation 1.5 μm and about 0.16 for the taper fiber with the taper deformation 1.0 μm. Many transmission peaks and dips exist, resulting from the light interference enhancement and interference destruction. The transmission contour is same for the no taper, one taper and two taper fiber and transmission peak positions shift for the tapered fiber. The transmission peak position is at about 0.667 μm for the no tapered fiber, 0.665 μm for the one tapered fiber and 0.662 μm for the two tapered fiber. The sensitivity of the tapered fiber is about 1.59e-3 nm μm-1.

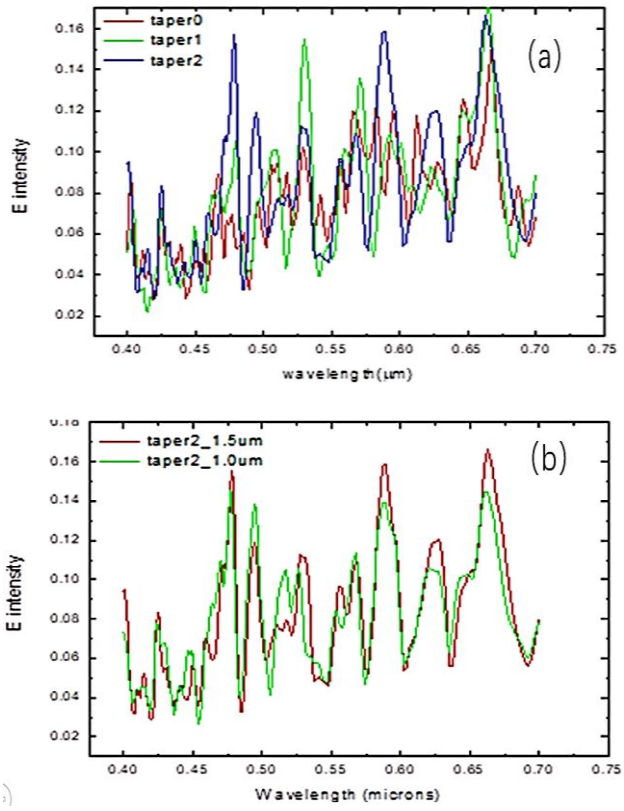

Fig. 2. (a) The simulated transmission spectra for the fiber with no, one and two deformations. The diameter of the fiber core is 3 μm and the diameter of the fiber shell is 6 μm. The thickness of the taper core is 1.5 μm and that of the taper shell is 3 μm. (b) The simulated transmission spectra for the fiber with two tapers. The thickness of one taper core at the entrance is 1.5 μm and 1.0 μm are changeable (color online)

Meanwhile, we have simulated the transmission spectra for the two tapered fiber with the taper deformation changing from 1.5 μm to 1.0 μm in the visible wavelength range by FDTD shown in Fig. 2(b). Many transmission peaks and dips exist in the transmission spectra, which result from the two light's interference reflected by the entrance and the outlet. The transmission contour is same for the two tapered fiber with different taper deformation. The transmission peak positions will shift to the short wavelength when the taper deformation changing from 1.5 μm m to 1.0 μm. The transmission peak position is at about 0.662 μm for the taper deformation 1.5 μm and about 0.661 μm for the taper deformation 1.0 μm. The sensitivity of the two tapered fiber on the thickness of the deformation is about 2.91e-3 nm μm -1.

The electric field distributions along XOZ plane at the wavelength 0.667 μm for the no tapered fiber are shown in Fig. 3(a), at the wavelength 0.665 μm for the one tapered fiber are shown in Fig. 3(b), at the wavelength 0.662 μm for the two tapered fiber with taper deformation 1.5 μm are shown in Fig. 3(c) and at the wavelength 0.661 μm for the two tapered fiber with taper deformation 1.0 μm are shown in Fig. 3(d). These electric field distributions shown in Fig. 3 are corresponding to the transmission peaks in the transmission spectra shown in Fig. 2. The light is incident in z-axis and polarized in x-axis. Better electric field localization and the electric field oscillation structures exist in the electric field distribution. The electric field mainly localized in the 200 nm and about 1μm apart from the outlet of the fiber which resulted from the electric field self focus at the outlet. The transmission light can achieve larger enhancement, which is about 60 times for the no-tapered fiber and about 30 times for the tapered fiber than the incident electric field. There is no more electric field loss for the no-tapered fiber than that of the tapered fiber. These structures can apply to the electric field enhancement and Raman scattering enhancement. The electric field along the fiber is single mode almost in the fiber core in 500 nm. The light propagates along the fiber core and total reflection by the side wall of the fiber. There is interference structure resulting from the two light's interference and apparent interference stripes exist in the electric field distributions. Meanwhile, the apparent interference enhancement and interference destruction exist in the electric field distributions images. The interference structure is pure for the no tapered fiber and it changes to be complicated for the tapered fiber. Meanwhile, there is multimode in the xoz plane along the fiber for the one tapered and two tapered fiber shown in Figs. 3(b)-3(d).

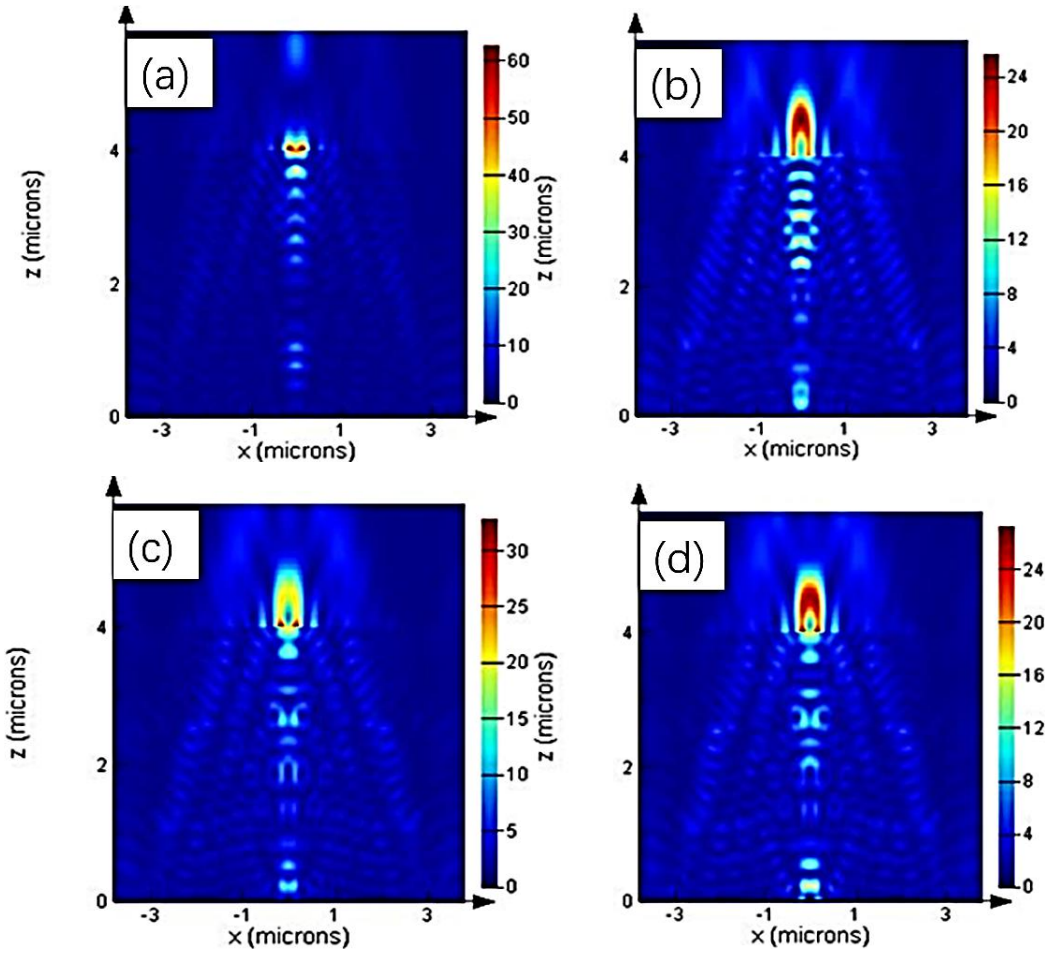

Fig. 3. Simulated the electric field distribution for the fiber with none, one, and two deformations at (a) the wavelength 0.667 μm, (b) 0.665 μm and (c) 0.662 μm respectively. The simulated electric field distribution for the two deformation structures with the first taper width 1.0 μm at the wavelength 0.661 μm (d) (color online)

We have also simulated the transmission spectra for the one tapered fiber with the different taper shell refractive in the visible wavelength range by use of FDTD shown in Fig. 4(a). The taper size is depicted above, which is composed of the shell and core structure. The taper shell refractive changes from 1.64 to 1.33 and the fiber core refractive is still 1.645. There are many transmission peaks and dips in the transmission spectra in the wavelength range from 0.4 μm to 0.7 μm. The transmission contour is same for the tapered fiber with different taper shell refractive. The transmission amplitude can achieve about 0.16, which is large for the light communication. The transmission peaks shift to the short wavelength when the taper shell refractive changes from 1.64 to 1.33. The transmission peak position for the tapered fiber with taper shell refractive 1.64 is at the wavelength 0.665 μm and it for the taper shell refractive 1.33 is at the wavelength 0.661 μm. The sensitivity for the one tapered fiber is about 12.3 nm·RIU-1, which can extensively apply to the bio-chemical detection. The electric field distributions along XOZ plane for the one tapered fiber are simulated by use of FDTD shown in Figs. 3(b) and 3(c). The electric field is at the wavelength 0.665 μm for the one tapered fiber with taper shell refractive 1.64 and at the wavelength 0.661 μm for the taper shell refractive 1.33. The electric field distributions are corresponding to the transmission peak in the transmission spectra. The electric field is incident in z-axis and polarized in x-axis. Better electric field localization and electric field enhancement are shown in the electric field distribution images. The electric field can localize in 200 nm and in one micro apart from the outlet of the fiber. The electric field localization results from the self focus effect. The electric field enhancement can achieve about 20 times than the incident electric field. Apparent interference structures exist

in the electric field distribution images, which result from the interaction of the electric field reflected by the taper and the outlet of the tapered fiber. The interference period is about 0.3 μm.

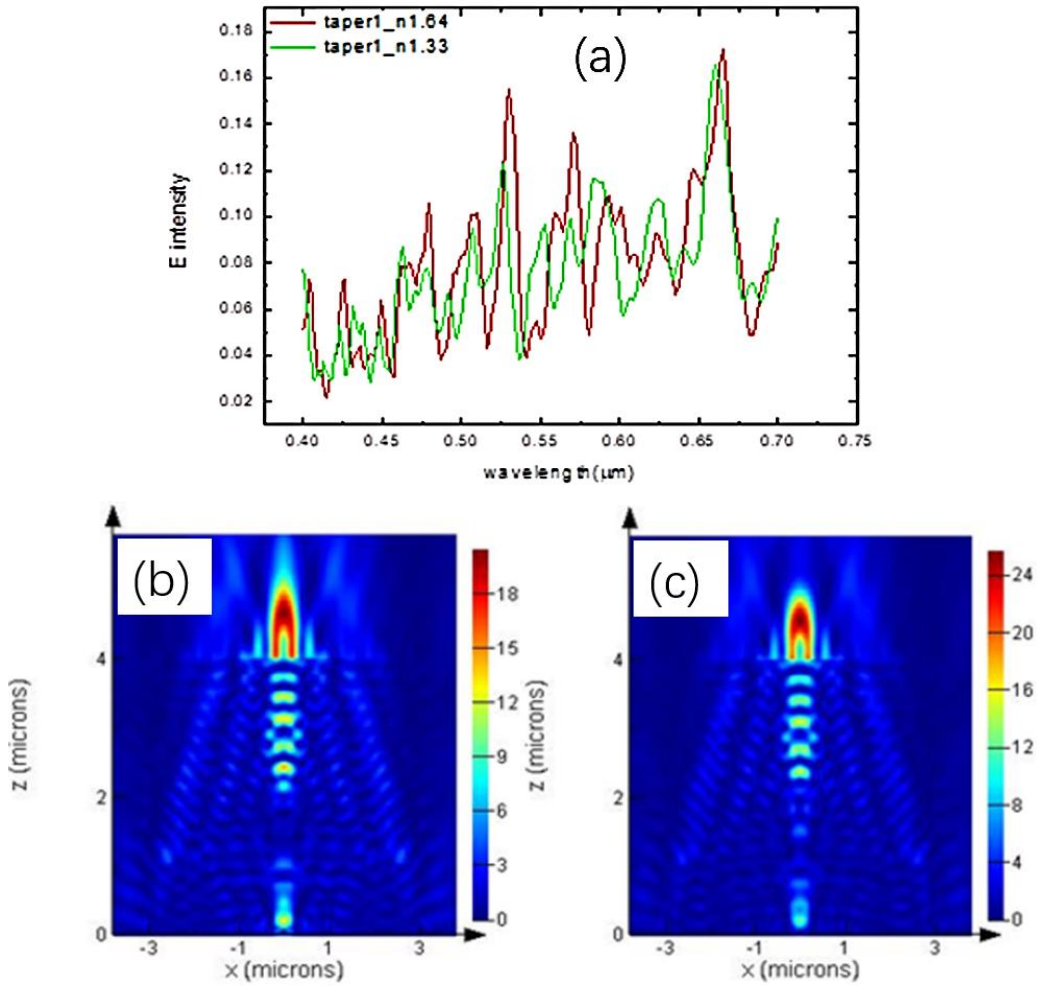

Fig. 4. (a) The simulated transmission spectra for the fiber with one taper by FDTD methods and the refractive of the taper shell structure is changeable, which changes from 1.64 to 1.33. (b) The simulated electric field distribution of the one tapered fiber with the taper shell refractive 1.33 at the wavelength 0.660 μm. (c) The simulated electric field distribution of the one tapered fiber with the taper shell refractive 1.64 at the wavelength 0.665 μm (color online)

We have simulated the transmission spectra for the two tapered fiber with taper shell refractive 1.64 and 1.33 by use of FDTD shown in Fig. 5(a). The transmission contours are same for the two tapered fiber with different taper shell refractive. There are many transmission peaks and dips in the transmission spectra in the wavelength range from 0.4 μm to 0.7 μm shown in Fig. 5(a). These transmission peaks result from the interference enhancement of the light reflected by the taper and the outlet of the fiber. The transmission peak positions will shift to the long wavelength when the taper shell refractive changes from 1.33 to 1.64. The transmission peak for the taper shell refractive 1.64 is at the wavelength 0.662 μm and it is for the taper shell refractive 1.33 at the wavelength 0.655 μm. The transmission amplitude can achieve about 0.16. We also simulated the transmission spectra of the two tapered fiber with taper shell refractive changing from 1.64 to 1.0. Transmission peaks and dips exist in the transmission spectra and the transmission peaks will shift to the long wavelength for the refractive changing larger. The transmission peak positions to the taper shell refractive are shown in Fig. 5(b). The transmission peak positions shift to the long wavelength when the refractive changing from 1.0 to 1.64. The sensitivity is about 50 nm RIU-1, which is

sensitive for the bio-chemical detection. Meanwhile, the sensitivity for the two tapered fiber is higher than that of the one tapered fiber.

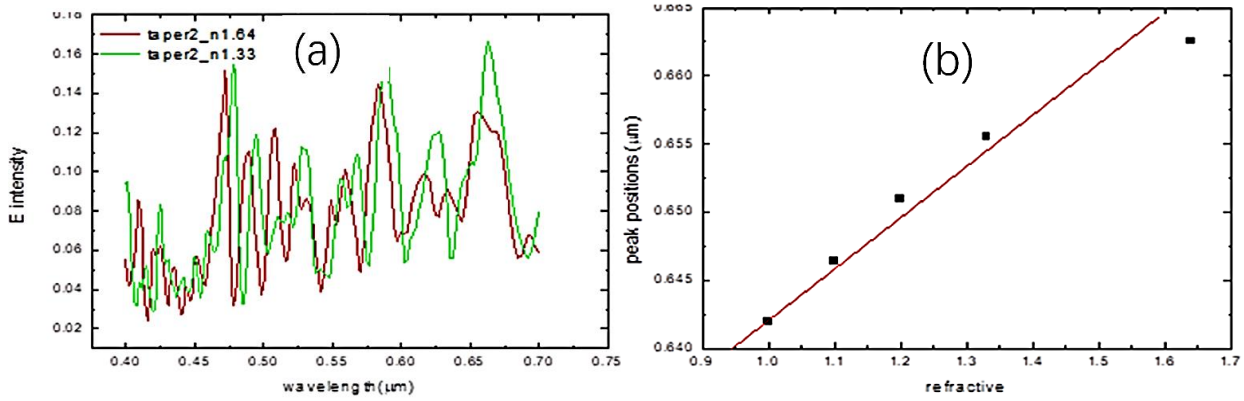

Fig. 5. (a) The simulated transmission spectra for the fiber with the two deformation have different shell refractive1.64 and 1.33 respectively. (b) The transmission peak positions for the fiber with two deformation have different refractive changed from 1.64 to 1.0 (color online)

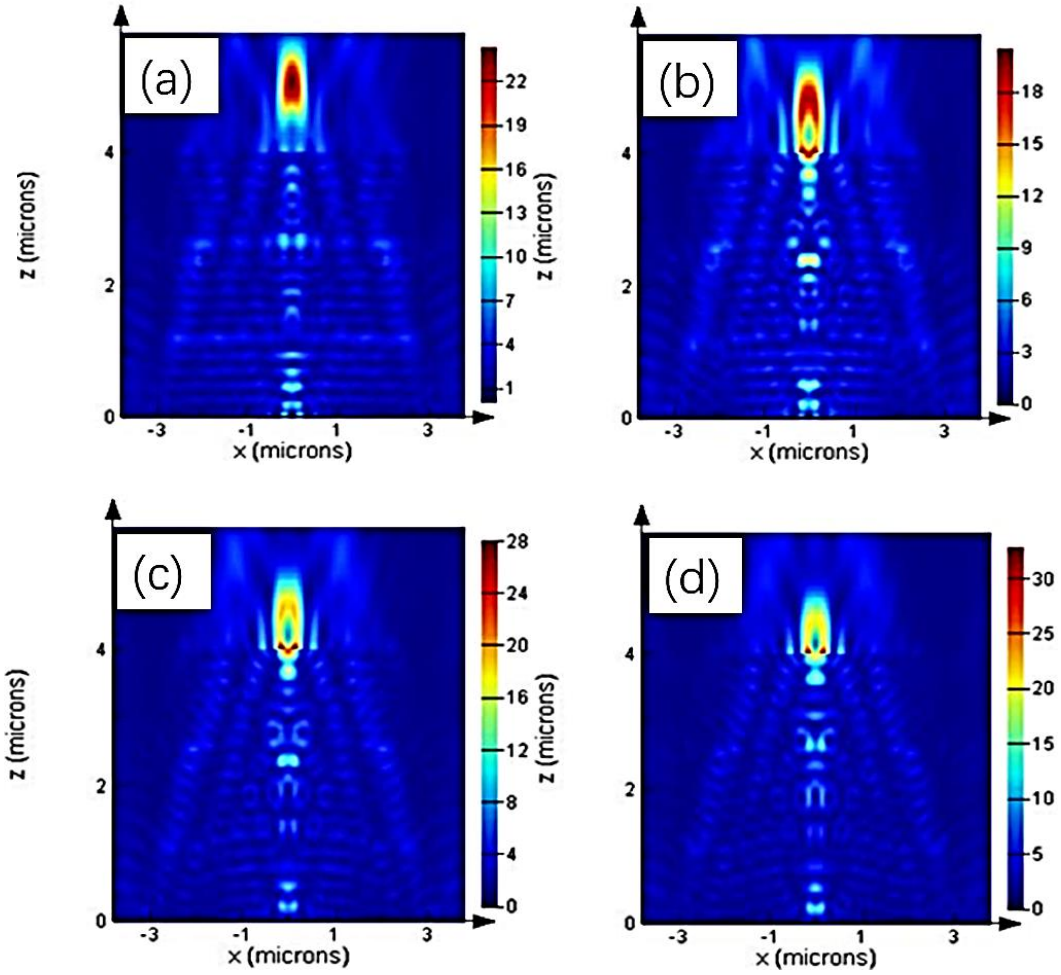

Fig. 6. Simulated the electric field distribution for the fiber with two deformation have the shell structure refractive 1.0 at the wavelength 0.641 μm (a), 1.2 at the wavelength 0.652 μm (b), 1.33 at the wavelength 0.655 μm (c) and 1.64 at the wavelength 0.652 μm (d) respectively (color online)

The electric field distributions in the XOZ plane for the two tapered fiber are at the wavelength 0.642 μm for the taper shell refractive 1.0 in Fig. 6(a), at the wavelength 0.651 μm for the taper shell refractive 1.2 in Fig. 6(b), at the wavelength 0.655 μm for the taper shell refractive 1.33 in Fig. 6(c), and at the wavelength 0.662 μm for the taper shell refractive 1.64 in Fig. 6(d). These electric field distributions are corresponding to the transmission peak in the transmission spectra shown in Fig 5(a). There is interference structure in the electric field distribution and light focuses in one micro apart from the fiber outlet. Better electric field localization and larger electric field enhancement exist in the electric field distribution images. The electric field can achieve about 30 times than the incident electric field. The first taper is at the 1.0 μm and the second taper is at about 2.3 μm apart from the entrance of the two tapered fiber. The interference structure is apparent, which result from the interaction of the light reflected by the two tapers. There are six interference stripes between the two tapers for the taper shell refractive 1.0. Meanwhile, there is high order modes in the electric field distribution images for the two tapered fiber and base mode exist in the electric field distribution for the common fiber. There is also better electric field localization in the tapered fiber core and in about 300 nm.

3. Conclusion

The simulated transmission spectra for the tapered fiber by use of FDTD in the visible wavelength range are presented. The transmission peak positions shift to the shorter wavelength when the taper number increases and the taper deformation gets larger. The sensitivity to the deformation is about 1.59e-3 nm·μm -1, which can be extensively applied to the sensing and physical test. We have also simulated the transmission spectra by use of FDTD for the tapered fiber with different taper shell refractive indices. The sensitivity to the taper shell refractive is about 50 nm·RIU-1 for the two tapered fiber and about 12.3 nm RIU-1 for the one tapered fiber. These structures can be applied to the bio-chemical detection. There is interference structure in the electric field distribution and it is apparent for the larger taper refractive difference and more taper numbers.

Acknowledgements

This research was supported by the National Natural Science Foundation of China (Nos.61178010 and 10805006), the Fundamental Research Funds for the Central Universities(No.bupt2010zx04), the National Program for Basic Research in China Grant No. 2010CB923202.

References

[1] J. H. Amanda, Z. Shengli, C. S. George, P. V. D. Richard, Phys. Chem. B **108**, 109 (2004).

[2] L. Jiangyan, M. Haiqiang, Optik – International Journal for Light and Electron Optics **05**, 6419 (2013).

[3] L. Jiangyan, G. Lin, F. Jinxin, L. Zhiyuan, Chinese Phys. B **22**, 117302 (2013).

[4] L. Jiangyan, Q. Kangsheng, M. Haiqiang, Chinese Phys. B **23**, 106804 (2014).

[5] L. Jiangyan, H. Yi Lei, F. Jinxin, L. Zhiyuan, J. Appl. Phys. **107**, 073101 (2001).

[6] L. Jiang-Yan, L. Zhi-Yuan, Y. Hai-Fang, J. Ai-Zi, J. Appl. Phys. **104**, 114303 (2008).

[7] C. M. B. Cordeiro, E. M. D. Santos, C. H. B. Cruz, C. J. D. Matos, D. S. Ferreiia, Opt. Express **14**, 8403 (2006).

[8] G. Barton, M. A. V. Eijkelenborg, G. Henry, M. C. J. Large, J. Zagari, Opt. Fiber Technol. **10**, 325 (2004).

[9] W. Wadsworth, N. Joly, J. Knight, T. Birks, F. Biancalana, P. L. Russel, Opt. Express **12**, 299 (2004).

[10] Z. Qi, N. Matsuda, J. Santos, H. K. Ito, A. Takatsu, K. Kenjo, Langmuir **19**, 214 (2003).

[11] R. F. Cregan, B. J. Mangan, J. C. Knight, T. A. Birks, P. S. J. Russell, P. J. Roberts, D. C. Allen, Science **285**, 1537 (1999).

[12] A. Argyros, M. A. V. Eijkelenborg, M. C. J. Large, I. M. Bassett, Opt. Lett. **31**, 172 (2006).

[13] T. Ritari, J. Tuominen, H. Ludvigsen, J. C. Petersen, H. Sorensen, T. P. Hansen, H. R. Simonsen, Opt.

Express **17**, 4080 (2004).
[14] J. M. Fini, Meas. Sci. Technol. **15**, 1120 (2004).
[15] W. K. A. M. Burns, C. A. Villarruel, Applied Optics **24**, 2753 (1985).
[16] J. D. L. A. W. M. Ilenry, Electron. Lett. **22**, 912 (1986).
[17] R. P. T. A. B. Kenny, K. P. Oakley, Electron. Lett. **27**, 1654 (1991).
[18] X. H. Zheng, J. Opt. Soc. Am. A **6**, 90 (1989).
[19] J. S. L. Bures, J. Lapierre, Applied Optics **22**, 1918 (1983).
[20] J. N. J. R. O. P. W. Dewynne, SIAM J. Appl. Math. **49**, 983 (1989).
[21] X. M. A. V. E. Shicheng, Journal of Lightwave Technology **25**, 1169 (2007).
[22] T. Daniel, D. C. Cassidy, Appl. Opt. **24**, 945 (1985).
[23] P. Russell, Science **299**, 358 (2003).
[24] J. Jensen, P. Hoiby, G. Emiliyanov, O. Bang, L. H. Pedersen, A. Bjarklev, Opt. Express **13**, 5883 (2005).
[25] P. S. Kumar, C. P. G. Vallabhan, V. P. N. Nampoori, V. N. S. Pillai, P. Radhakrishnan, J. Opt. A: Pure Appl. Opt. **4**, 247 (2002).
[26] P. J. Wiejata, P. M. Shankar, R. Mutharasan, Sens. Actuators B **96**, 315 (2003).
[27] C. M. B. Cordeiro, E. M. D. Santos, C. H. B. Cruz, C. J. D. Matos, D. S. Ferreira, Opt. Express **14**, 8403 (2006).

*Corresponding author: yanr163@163.com